

## EXACT SOLUTIONS FOR INTERFACIAL OUTFLOWS WITH STRAINING

LAWRENCE K. FORBES<sup>✉1</sup> and MICHAEL A. BRIDESON<sup>1</sup>

(Received 28 November, 2012; revised 4 September, 2013; first published online 5 June 2014)

### Abstract

In models of fluid outflows from point or line sources, an interface is present, and it is forced outwards as time progresses. Although various types of fluid instabilities are possible at the interface, it is nevertheless of interest to know the development of its overall shape with time. If the fluids on either side are of nearly equal densities, it is possible to derive a single nonlinear partial differential equation that describes the interfacial shape with time. Although nonlinear, this equation admits a simple transformation that renders it linear, so that closed-form solutions are possible. Two such solutions are illustrated; for a line source in a planar straining flow and a point source in an axisymmetric background flow. Possible applications in astrophysics are discussed.

2010 *Mathematics subject classification*: 76B07.

*Keywords and phrases*: closed-form solution, hydrodynamics, interfacial fluid flow, straining flow.

### 1. Introduction

This paper considers a simple idealized model of fluid flow from a source, modelled as a singularity, in the presence of an external straining flow. The fluid in the bubble surrounding the source is of density  $\rho_1$  and the outer ambient fluid has density  $\rho_2$  and, consequently, there is an interface between them. Each fluid is regarded as incompressible and inviscid and, since there is a source present, the interface must move outwards with time, as it necessarily encloses an ever-increasing volume. If the surrounding fluid simply moves outwards passively, due to the source, then the shape adopted by the interface is at once obvious; it is a circular cylinder for planar flow or an expanding sphere for a point source in three-dimensional space. However, when an external straining flow is also present, the shape adopted by the interface is no longer a trivial matter. This paper presents a simple, closed-form approach for determining that shape, under the assumption that the two fluids have nearly equal densities.

---

<sup>1</sup>School of Mathematics and Physics, University of Tasmania, Private Bag 37, Hobart, Tasmania, Australia; e-mail: [Larry.Forbes@utas.edu.au](mailto:Larry.Forbes@utas.edu.au), [Michael.Brideson@utas.edu.au](mailto:Michael.Brideson@utas.edu.au).

© Australian Mathematical Society 2014, Serial-fee code 1446-1811/2014 \$16.00

The original motivation for considering this problem comes from astrophysics, in which expanding bubbles are observed about objects such as young stars. While these are complex environments, involving gases, shocks and magnetic fields, the fundamental question is to determine the overall shape adopted by the bubble and the factors that influence it. In particular, it is of interest to know to what extent the shape of the bubble is determined by the motion of the surrounding interstellar medium.

Considerable research has been devoted to this question, and the article by Bally et al. [2] gives an experimental overview of the shapes of structures within the Orion nebula, caused in part by the interaction of fluid jets with their environment. Perucho and Bosch-Ramon [16] carried out numerical simulations of the interaction of astrophysical jets with stellar cross winds, and Lebedev et al. [12] undertook a high-energy laboratory experimental investigation of the deflection of a hypersonic jet by a cross wind, with the intention of accounting for the similar phenomenon in astrophysics. An analytical model of the curving of a jet in a stellar cross wind has been presented by Raga et al. [17].

In a number of applications, such as underwater explosions, astrophysics [14] and the inertial confinement of plasmas as discussed by Epstein [6], the densities of the inner and outer fluids may be very nearly equal, so that  $\rho_2/\rho_1 \approx 1$ . However, when the two densities are not precisely equal, various types of additional instabilities may be present at the interface, and these can have a strong effect on the evolution of its shape. If the outer fluid is heavier,  $\rho_2 > \rho_1$ , in planar cylindrical flow with gravity directed radially inwards, then a type of Rayleigh–Taylor instability is possible, and this can result in the formation of fingers at the interface. A linearized analysis of these structures is presented by Mikaelian [15]. In such cases, the curvature of the interface can further destabilize the flow by means of the so-called Bell–Plesset effect (see the article by Epstein [6]), and Forbes [7] has shown how the large-amplitude fingers may develop into over-turning plumes.

In three-dimensional axisymmetric outflow from a point source, the situation is similar, but with an important additional feature. The spherical interface surrounding the source may again be subject to instabilities, and these are sensitive to both the density ratio  $\rho_2/\rho_1$  and the mode number of the disturbance. In particular, the lowest mode  $n = 1$  is the most unstable, having the fastest growth rate in linearized theory. This was shown recently by Forbes [8], although the equation from which this conclusion derives was given previously by Mikaelian [15]. This means that, after sufficient time has elapsed, the outflow ought to be dominated by the lowest mode, so that a one-sided outflow would be observed, regardless of the initial perturbation to the interface. There is, in fact, some computational evidence [8, 13] in addition to experimental observation [3] to support these predicted one-sided outflows. Nevertheless, it is also the case that two-sided, bi-polar outflows are commonly observed in astrophysics (see the book by Stahler and Palla [18]). This raises the question as to whether such flows might be the result of the motion of the fluid in the surrounding medium, at least when the density ratio is close to unity, and this is the

motivation for the present study. Here, we consider the simplest situation, in which the additional background motion is a simple straining flow.

In the planar cylindrical case in Section 2 and the three-dimensional axisymmetric situation encountered in Section 3, it will be seen that the approximate models give rise to a partial differential equation (PDE) of the general form

$$\frac{\partial u}{\partial t} + f(x, t) \frac{\partial u}{\partial x} + g(x, t)u = h(x, t)u^n, \quad (1.1)$$

in which the exponent  $n$  is neither 0 nor 1. This is, therefore, a nonlinear PDE for the quantity  $u(x, t)$ . There is, however, a close analogy between this *partial* differential equation (1.1) and the famous Bernoulli *ordinary* differential equation given in textbooks such as Giordano and Weir [9]. An engaging discussion of the history of the Bernoulli equation is also given in the monograph by de Mestre [5, Chapter 3]. Equation (1.1) can be reduced to a linear PDE by the power-law change of variable  $u(x, t) = [Z(x, t)]^\alpha$ , if the transformation parameter is chosen to be  $\alpha = 1/(1 - n)$ , analogously to the famous ordinary differential equation. For this reason, we refer here to (1.1) as a ‘Bernoulli PDE’. The resulting linear equation then becomes

$$\frac{\partial Z}{\partial t} + f(x, t) \frac{\partial Z}{\partial x} + (1 - n)g(x, t)Z = (1 - n)h(x, t),$$

and a closed-form solution is often available by means of Fourier series or the method of characteristics (see the book by Haberman [10]). Solutions obtained by this approach will be presented in both the planar and axisymmetric situations in Sections 2 and 3, and in each case the nonlinear PDE will be transformed to a linear equation which is then solved completely using a generalized separation of variables technique that derives from the method of characteristics. Some interface shapes will be illustrated in each case, and some concluding remarks given in Section 4.

## 2. Line source in planar straining flow

This section considers a system of two inviscid, immiscible and incompressible fluids separated by a sharp interface, in planar (two-dimensional) flow parallel to the  $x$ - $y$  plane. The inner fluid has density  $\rho_1$  and initially forms a circle centred at the origin. Cylindrical polar coordinates will be used from now on, and they are related to the Cartesian system by means of the usual relations  $x = r \cos \theta$ ,  $y = r \sin \theta$ . There is an outer fluid of density  $\rho_2$  and it is separated from the inner fluid by an interface located at  $r = R(\theta, t)$ . The geometry in this planar case is illustrated in Figure 1. A line sink of strength  $m$  is located at the origin, within the region occupied by the inner fluid, and there is also a straining flow present, corresponding effectively to two fluid streams moving parallel to the  $x$ -axis towards the origin and then flowing outwards up or down the  $y$ -axis.

Because each fluid is incompressible and inviscid, it therefore flows irrotationally. Accordingly, the velocities  $\mathbf{q}_1$  and  $\mathbf{q}_2$  in the inner and outer fluids, respectively, can each be written in terms of scalar velocity potential functions  $\Phi_1$  and  $\Phi_2$  by means of

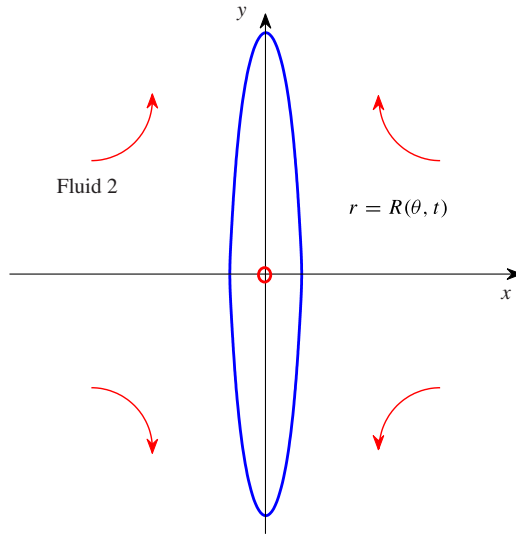


FIGURE 1. A sketch of the flow configuration for the planar straining flow problem. A line source of strength  $m$  is present at the origin, and the interface  $r = R(\theta, t)$  is taken from an actual solution with  $m/(a^2A) = 0.5$ , at dimensionless time  $At = 0.5$ .

the relations  $\mathbf{q}_j = \text{grad}\Phi_j = u_j\mathbf{e}_r + v_j\mathbf{e}_\theta$  for  $j = 1, 2$ . The velocity potential in each fluid must satisfy Laplace’s equation

$$\nabla^2\Phi_j = \frac{1}{r} \frac{\partial}{\partial r} \left( r \frac{\partial \Phi_j}{\partial r} \right) + \frac{1}{r^2} \frac{\partial^2 \Phi_j}{\partial \theta^2} = 0 \tag{2.1}$$

in its domain. There is also a set of two kinematic boundary conditions to be applied at the interface  $r = R(\theta, t)$ . These state that neither fluid is free to cross the interface and enter the other fluid, and may be expressed as

$$u_j = \frac{\partial R}{\partial t} + \frac{v_j}{R} \frac{\partial R}{\partial \theta} \quad \text{on } r = R(\theta, t) \tag{2.2}$$

for  $j = 1, 2$ . In addition, there is a dynamic boundary condition at the interface  $r = R(\theta, t)$ , and it is derived from the fact that the pressure must be continuous on crossing the interface.

It is now assumed that density differences between the two fluids may be ignored, so that  $\rho_1 = \rho_2$ . The velocity potentials in each fluid are then given, and consist of a contribution from a source at the origin and a planar straining flow at infinity. Thus,

$$\Phi_1 = \Phi_2 = \frac{m}{2\pi} \log r - Ar^2 \cos(2\theta). \tag{2.3}$$

Here,  $m$  is the strength (volume per time per width) of the line source, and the constant  $A$  gives the strength of the straining flow; it has units of 1/time. These velocity

potentials (2.3) satisfy Laplace’s equation (2.1), and result in velocity components

$$\begin{aligned} u_1 = u_2 &= \frac{m}{2\pi r} - 2Ar \cos(2\theta), \\ v_1 = v_2 &= 2Ar \sin(2\theta). \end{aligned} \tag{2.4}$$

With the velocity vectors and densities equal in the two fluid regions, the dynamic boundary condition of continuous pressure across the interface is satisfied identically, and so will not be considered further here.

When the velocity components (2.4) are substituted into the kinematic boundary conditions (2.2), there results at once the partial differential equation

$$\frac{\partial R}{\partial t} + 2A \sin(2\theta) \frac{\partial R}{\partial \theta} + 2A \cos(2\theta)R = \frac{m}{2\pi R}$$

for the shape of the interface  $r = R(\theta, t)$ . This is immediately seen to be a ‘Bernoulli’ PDE, in the form of (1.1). Although it is nonlinear, this equation can be transformed to a linear PDE by the change of variable  $R = Z^{1/2}$ , as explained in Section 1.

The new equation for the variable  $Z(\theta, t)$  now becomes

$$\frac{\partial Z}{\partial t} + 2A \sin(2\theta) \frac{\partial Z}{\partial \theta} + 4A \cos(2\theta)Z = \frac{m}{\pi} \tag{2.5}$$

in this planar case. It is assumed here that the interface starts as a cylinder of radius  $a$  and, thus, the initial condition for the new transformed variable is

$$Z(\theta, 0) = a^2. \tag{2.6}$$

A closed-form solution for the transformed PDE (2.5) and its initial condition (2.6) is now derived, based on the method of characteristics (see Haberman [10, page 319]). The physical characteristics for the PDE (2.5) are curves along which

$$\frac{d\theta}{dt} = 2A \sin(2\theta),$$

which has solutions

$$\frac{\cos \theta}{\sin \theta} e^{4At} = C$$

for arbitrary constants  $C$ . Accordingly, a solution is sought in the form

$$Z(\theta, t) = F(\theta)G\left(\frac{\cos \theta}{\sin \theta} e^{4At}\right) + P(\theta), \tag{2.7}$$

in which the functions  $F$ ,  $G$  and  $P$  are to be determined. This may be regarded as a generalization of the usual separation of variables technique. It follows that the differential equation (2.5) may be satisfied identically by choosing

$$\begin{aligned} 2A \sin(2\theta)F'(\theta) + 4A \cos(2\theta)F(\theta) &= 0, \\ 2A \sin(2\theta)P'(\theta) + 4A \cos(2\theta)P(\theta) &= m/\pi, \end{aligned} \tag{2.8}$$

leaving the remaining function  $G$  arbitrary so far. These ordinary differential equations (2.8) are easily solved using an integrating factor and, when combined with the general form (2.7), they give rise to

$$Z(\theta, t) = \frac{1}{\sin(2\theta)} \left[ G\left(\frac{\cos \theta}{\sin \theta} e^{4At}\right) + \frac{m\theta}{2\pi A} \right] \quad (2.9)$$

without any loss of generality. Finally, the initial condition (2.6) must be imposed on the solution (2.9), and it yields a general form for the remaining function  $G$ . The result is

$$G\left(\frac{\cos \theta}{\sin \theta}\right) = -\frac{m\theta}{2\pi A} + a^2 \sin(2\theta).$$

In order to see the general form of the function  $G$  for arbitrary argument, it is convenient to introduce the variable  $\xi = \cot \theta$ , from which it then follows that

$$G(\xi) = -\frac{m}{2\pi A} \arctan\left(\frac{1}{\xi}\right) + \frac{2a^2\xi}{\xi^2 + 1}.$$

Consequently, the final form of the solution (2.9) is

$$Z(\theta, t) = \frac{a^2 e^{-4At}}{(\cos^2 \theta + \sin^2 \theta e^{-8At})} + \frac{m}{2\pi A \sin(2\theta)} [\theta - \arctan(\tan \theta e^{-4At})]. \quad (2.10)$$

Various different forms of this solution (2.10) have been derived, although most of these will not be discussed here. However, it has been verified directly that the result (2.10) does indeed satisfy the linear PDE (2.5). For ease of evaluation, it is convenient to write  $\theta = \arctan(\tan \theta)$  in the first term in parentheses of the second term on the right-hand side of (2.10), and then make use of the result in Abramowitz and Stegun [1, page 80, Formula 4.4.34] for the difference of two arctangents. This yields

$$Z(\theta, t) = \frac{a^2 e^{-4At}}{(\cos^2 \theta + \sin^2 \theta e^{-8At})} + \frac{m}{2\pi A \sin(2\theta)} \arctan\left(\frac{[1 - e^{-4At}] \sin \theta \cos \theta}{\cos^2 \theta + \sin^2 \theta e^{-4At}}\right). \quad (2.11)$$

This form makes the periodicity of the solution in the coordinate  $\theta$  more apparent. In addition, the solution (2.11) shows that the potential singularities whenever  $\sin(2\theta) = 0$  are completely removable. The radius function  $R(\theta, t)$  is finally obtained from the solution (2.11) using the transformation  $R = Z^{1/2}$ .

This solution is illustrated in Figure 2. In this diagram, the source strength has been set at the (dimensionless) value  $m/(a^2 A) = 0.5$ , and the evolution of the interface  $R(\theta, t)$  is displayed at six (dimensionless) times  $At = 0, 0.1, 0.2, \dots, 0.5$ . The initial circular cylinder  $R(\theta, 0)/a = 1$  is visible at the centre of the diagram and, as the interface evolves, it develops an elongated shape up and down the  $y$ -axis, as might be expected on the basis of the background flow velocity vector (2.4). Similar results are obtained at other source strengths, although the time taken for a particular outflow structure to be achieved may vary with  $m$ .

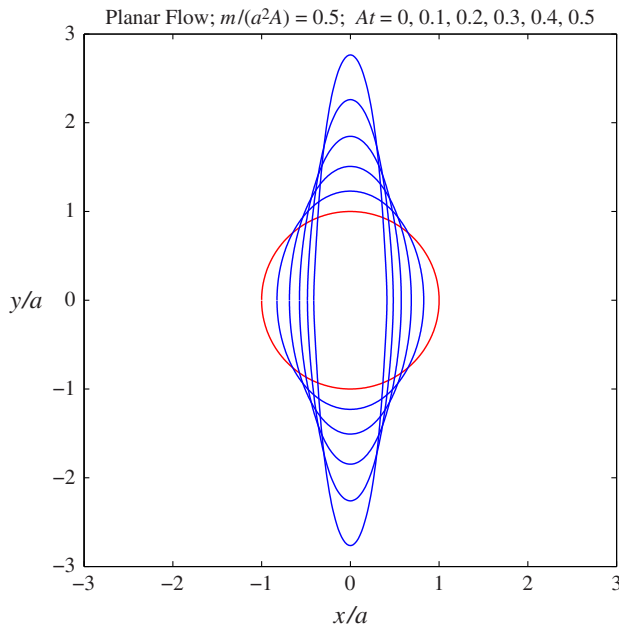


FIGURE 2. Representative solutions for the interface shape in planar flow. Here, the axes are scaled relative to the initial radius  $a$  of the cylinder. Solutions are shown for the dimensionless outflow rate  $m/(a^2A) = 0.5$  and the six dimensionless times  $At = 0, 0.1, \dots, 0.5$ .

### 3. Point source in axisymmetric straining flow

It is possible to carry out the corresponding solution for axisymmetric flow from a point source in an ambient straining flow. The density ratio between the two fluids is again taken to be  $\rho_2/\rho_1 = 1$ , and now the appropriate velocity potentials in three-dimensional geometry are

$$\Phi_1 = \Phi_2 = -\frac{m}{4\pi r} + Ar^2P_2(\cos \phi). \quad (3.1)$$

In this expression, spherical polar coordinates have been used, rather than the cylindrical polars in Section 2, so that  $r = \sqrt{x^2 + y^2 + z^2}$  and  $z = r \cos \phi$ . The geometry is assumed to be axisymmetric, so that there is now no longer any dependence on the azimuthal angle  $\theta$  in Section 2; instead, the elevation angle  $\phi$ , measured downwards from the  $z$ -axis, is the only angle of importance. The source strength is again denoted by the symbol  $m$ , and has units of volume per time. The straining rate is  $A$  (in units of 1/time), and the function  $P_2$  is the Legendre polynomial of second order (see Abramowitz and Stegun [1, page 333]). These potentials (3.1) are solutions to Laplace's equation in spherical polar coordinates, and the velocity vector now takes the form  $\mathbf{q}_j = \text{grad}\Phi_j = u_j\mathbf{e}_r + w_j\mathbf{e}_\phi$  in each fluid region,  $j = 1, 2$ , for which the velocity

components are

$$\begin{aligned} u_1 = u_2 &= \frac{m}{4\pi r^2} + 2ArP_2(\cos \phi), \\ w_1 = w_2 &= -ArP_2'(\cos \phi) \sin \phi. \end{aligned} \quad (3.2)$$

The kinematic conditions in spherical polar coordinates are

$$u_j = \frac{\partial R}{\partial t} + \frac{w_j}{R} \frac{\partial R}{\partial \phi} \quad \text{on } r = R(\phi, t) \quad (3.3)$$

for  $j = 1, 2$ , similar to their counterparts (2.2) in planar geometry. When the velocity components (3.2) are used in these conditions (3.3), it follows that the interface shape  $R = R(\phi, t)$  is obtained as the solution to the PDE

$$\frac{\partial R}{\partial t} - 3A \cos \phi \sin \phi \frac{\partial R}{\partial \phi} - A(3 \cos^2 \phi - 1)R = \frac{m}{4\pi R^2}.$$

This is again a ‘Bernoulli’ partial differential equation, of the same form as (1.1). It follows from Section 1 that it may be reduced to a linear PDE by the change of variable  $R = Z^{1/3}$ , and the equation for the new variable  $Z$  becomes

$$\frac{\partial Z}{\partial t} - 3A \cos \phi \sin \phi \frac{\partial Z}{\partial \phi} - 3A(3 \cos^2 \phi - 1)Z = \frac{3m}{4\pi}. \quad (3.4)$$

At time  $t = 0$ , the interface is assumed to be a sphere of radius  $a$ , so that the appropriate initial condition is

$$Z(\phi, 0) = a^3. \quad (3.5)$$

A closed-form solution is also available to this axisymmetric problem (3.4) and (3.5), using the method of characteristics to suggest a generalized separation of variables argument, similar to (2.7) in the planar case. The physical characteristics of (3.4) are obtained in a similar manner to Section 2, and they are now given as solutions to the ordinary differential equation

$$\frac{d\phi}{dt} = -3A \cos \phi \sin \phi.$$

This has general solutions

$$\frac{\cos \phi}{\sin \phi} = C e^{3At}$$

for arbitrary constants  $C$  and, therefore, a solution to the linear PDE (3.4) is sought in the general form

$$Z(\phi, t) = F(\phi)G\left(\frac{\cos \phi}{\sin \phi} e^{-3At}\right) + P(\phi), \quad (3.6)$$

in which, again, the three functions  $F$ ,  $G$  and  $P$  are to be determined. By substituting this form (3.6) into the linear PDE (3.4), the equation may be satisfied for an arbitrary function  $G$  by choosing

$$\begin{aligned} A \cos \phi \sin \phi F'(\phi) + A(3 \cos^2 \phi - 1)F(\phi) &= 0, \\ A \cos \phi \sin \phi P'(\phi) + A(3 \cos^2 \phi - 1)P(\phi) &= -\frac{m}{4\pi}. \end{aligned} \quad (3.7)$$

These ordinary differential equations (3.7) are linear and can be solved with an integrating factor. As a result, the assumed form (3.6) of the solution becomes

$$Z(\phi, t) = \frac{1}{\cos \phi \sin^2 \phi} \left[ G \left( \frac{\cos \phi}{\sin \phi} e^{-3At} \right) + \frac{m}{4\pi A} \cos \phi \right]. \tag{3.8}$$

This form of the solution (3.8) is now required to satisfy the initial condition (3.5), and this leads at once to the statement

$$G \left( \frac{\cos \phi}{\sin \phi} \right) = \cos \phi \left( a^3 \sin^2 \phi - \frac{m}{4\pi A} \right).$$

The change of variable  $\xi = \cot \phi$  gives the required form of the function  $G$  to be

$$G(\xi) = \frac{\xi}{\sqrt{1 + \xi^2}} \left( \frac{a^3}{1 + \xi^2} - \frac{m}{4\pi A} \right),$$

and this may now be combined with (3.8) to give the final form of the solution for  $Z$ . After some algebra, the result is found to be

$$Z(\phi, t) = \frac{a^3 e^{-3At}}{[\sin^2 \phi + \cos^2 \phi e^{-6At}]^{3/2}} + \frac{m}{4\pi A} \frac{(1 - e^{-6At})}{\sqrt{\sin^2 \phi + \cos^2 \phi e^{-6At}} \left[ \sqrt{\sin^2 \phi + \cos^2 \phi e^{-6At}} + e^{-3At} \right]}. \tag{3.9}$$

It has been checked that this function (3.9) does indeed satisfy the linear PDE (3.4), and the interface shape is recovered from the transformation  $R = Z^{1/3}$ .

It is evident from a comparison of this axisymmetric interface (3.9) with the planar result (2.11) that the different geometry gives at least qualitatively similar behaviour in the two different cases. This may be seen in Figure 3, where a representative solution is graphed at four different dimensionless times. Initially, the interface begins as a sphere, but is drawn into an elongated cigar-shaped object by the straining flow. Similar results are obtained at all source strengths  $m$ . Crowdy [4] also obtained comparable results for an interface in a straining flow, although in that case he considered a genuinely two-phase flow in a Hele–Shaw cell, so that the relation to the present results remains unclear.

To illustrate the three-dimensional nature of the interface in this case, two solutions are shown in Figure 4, for the same dimensionless value  $m/(a^3 A) = 5$  of the source strength. The diagram on the left is simply the initial sphere of radius  $R/a = 1$ , but the figure on the right shows the shape of the interface after dimensionless time  $At = 0.7$ . Both these pictures are drawn with the same scale and with equal intervals on all axes, so that the interfacial shapes are as they would actually appear.

### 4. Discussion and conclusion

The purpose of the present paper has been to examine a canonically simple model for outflow from a line or point source in a simple straining flow, as a

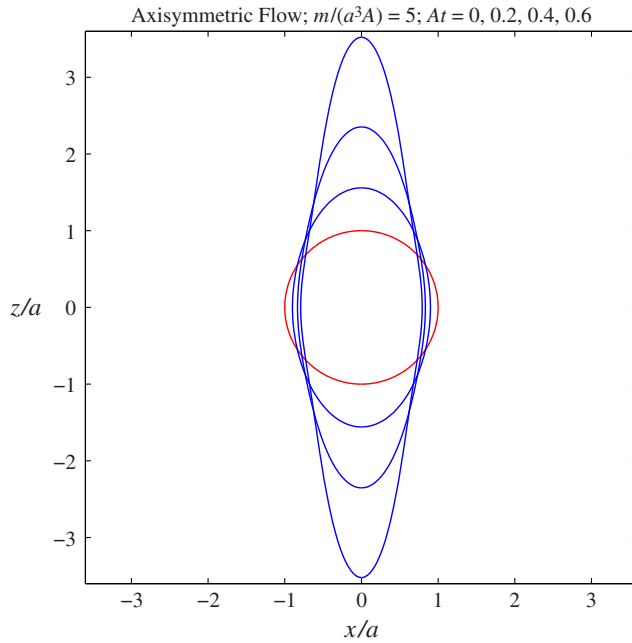


FIGURE 3. Representative solutions for the interface shape in axisymmetric flow. Here, the axes are scaled relative to the initial radius  $a$  of the sphere. Solutions are shown for the dimensionless outflow rate  $m/(a^3A) = 5$  and the four dimensionless times  $At = 0, 0.2, 0.4, 0.6$ .

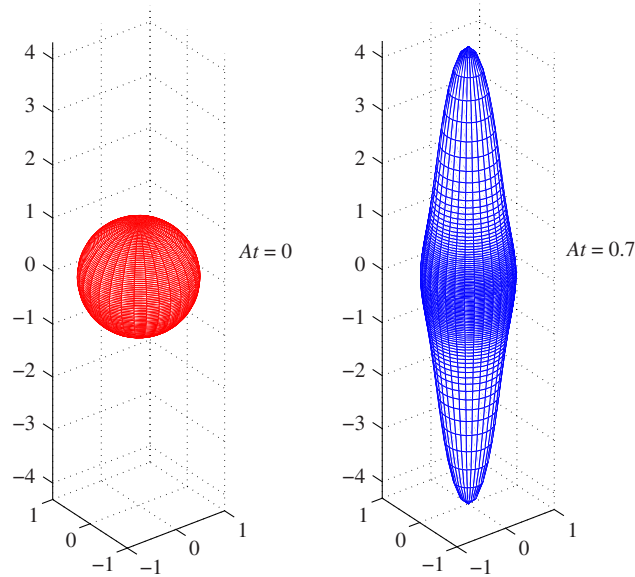


FIGURE 4. Two solutions for the interface shape in axisymmetric flow, for the case  $m/(a^3A) = 5$ . The solution on the left is the initial sphere of radius  $r/a = 1$ , and the solution on the right is the shape of the interface at dimensionless time  $At = 0.7$ .

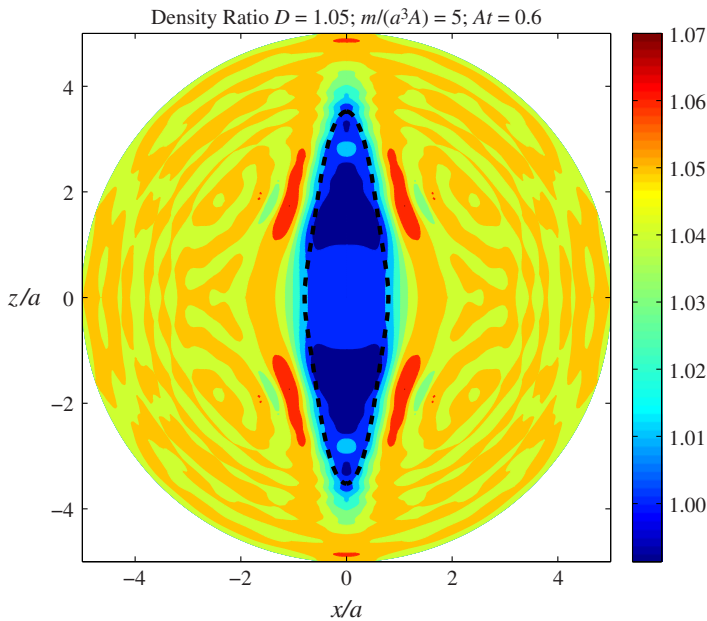


FIGURE 5. A comparison of the exact solution for axisymmetric outflow from a point source in a straining field with the results of a viscous simulation, at time  $At = 0.6$ . The exact solution (3.9) is drawn with a heavy dashed line, and is imposed over density contours for a viscous solution at the density ratio  $\rho_2/\rho_1 = 1.05$ . The dimensionless source strength is  $m/(a^3A) = 5$ .

first approximation for more complicated situations encountered in astrophysics, for example. Exact closed-form solutions have been found, analogously with the work of Kida [11] for a line vortex in a straining flow, or Crowdy [4] for flow in a Hele–Shaw cell. There are more general background straining flows, including situations in which the axisymmetric restriction of Section 3 is relaxed, which also lead to ‘Bernoulli’-type nonlinear PDEs of the form (1.1); these also are capable of solution in closed form, but are not discussed here.

In order to obtain the relatively simple, although nonlinear, partial differential equations that are capable of subsequent exact solution, it has been necessary to make the approximation  $\rho_2/\rho_1 = 1$  for the density ratio of the two fluids. The question then arises as to how useful the solutions in the present paper may be, in situations when the two fluids are of different densities.

This is clearly a much more difficult problem that goes far beyond the scope of the present investigation. However, we claim that the exact solutions presented here are nevertheless an indicative first-order approximation to the more complex situation in which the density ratio between the fluids differs from one, but is close to it. In support of this assertion, the numerical scheme in Forbes [8], which solves an approximate viscous model for axisymmetric outflow from a point source, has been modified to include an additional straining flow, and compared with the exact solution (3.9) after the transformation  $R = Z^{1/3}$  has been applied.

Figure 5 shows the interface obtained from the exact solution in Section 3 at dimensionless time  $At = 0.6$ , overlaid on the results of the viscous solution of Forbes [8] at that same time, with the straining field (3.2) added. The viscous simulation has been carried out for density ratio  $\rho_2/\rho_1 = 1.05$  so as to provide an approximate comparison with the exact solution of the present paper, which is indicated with a heavy dashed line in Figure 5. Contours of the density are shown for the viscous solution, so that the inner region has dimensionless density  $\rho = 1$  and the outer fluid has  $\rho = 1.05$ . Of course, the two solutions cannot be expected to be identical, since the density ratio differs in each case; nevertheless, the exact solution (3.9) lies fairly closely along the outer edge of the inner viscous region of the numerical simulation, along the contour  $\rho = 1$ . This indicates that the exact solutions in the present paper do indeed give a useful approximation to a problem of potential interest in astrophysics and underwater explosions. The solutions presented here may possibly serve as a basis for a perturbation analysis of the flow with  $\rho_2 \neq \rho_1$ , and this awaits future research.

### Acknowledgements

Comments and suggestions from two anonymous reviewers are gratefully acknowledged.

### References

- [1] M. Abramowitz and I. A. Stegun (eds), *Handbook of mathematical functions* (Dover, New York, 1972).
- [2] J. Bally, C. R. O'Dell and M. J. McCaughrean, "Disks, microjets, windblown bubbles, and outflows in the Orion nebula", *Astronom. J.* **119** (2000) 2919–2959; doi:10.1086/301385.
- [3] A. N. Chené and N. St-Louis, "Large-scale periodic variability of the wind of the Wolf–Rayet star WR 1 (HD 4004)", *Astrophys. J.* **716** (2010) 929–941; doi:10.1088/0004-637X/716/2/929.
- [4] D. G. Crowdy, "Exact solutions to the unsteady two-phase Hele–Shaw problem", *Quart. J. Mech. Appl. Math.* **59** (2006) 475–485; doi:10.1093/qjmam/hbl012.
- [5] N. de Mestre, *The mathematics of projectiles in sport*, Volume 6 of *Australian Mathematical Society Lecture Series* (Cambridge University Press, Cambridge, 1990).
- [6] R. Epstein, "On the Bell–Plesset effects: the effects of uniform compression and geometrical convergence on the classical Rayleigh–Taylor instability", *Phys. Plasmas* **11** (2004) 5114–5124; doi:10.1063/1.1790496.
- [7] L. K. Forbes, "A cylindrical Rayleigh–Taylor instability: radial outflow from pipes or stars", *J. Engrg. Math.* **70** (2011) 205–224; doi:10.1007/s10665-010-9374-z.
- [8] L. K. Forbes, "Rayleigh–Taylor instabilities in axi-symmetric outflow from a point source", *ANZIAM J.* **53** (2011) 87–121; doi:10.1017/S1446181112000090.
- [9] F. R. Giordano and M. D. Weir, *Differential equations: a modeling approach* (Addison-Wesley, Reading, MA, 1988).
- [10] R. Haberman, *Mathematical models: mechanical vibrations, population dynamics and traffic flow* (Prentice-Hall, Englewood Cliffs, NJ, 1977).
- [11] S. Kida, "Motion of an elliptic vortex in a uniform shear flow", *J. Phys. Soc. Japan* **50** (1981) 3517–3520; doi:10.1143/JPSJ.50.3517.
- [12] S. V. Lebedev, D. Ampleford, A. Ciardi, S. N. Bland, J. P. Chittenden, M. G. Haines, A. Frank, E. G. Blackman and A. Cunningham, "Jet deflection via crosswinds: laboratory astrophysical studies", *Astrophys. J.* **616** (2004) 988–997; doi:10.1086/423730.

- [13] R. V. E. Lovelace, M. M. Romanova, G. V. Ustyugova and A. V. Koldoba, “One-sided outflows/jets from rotating stars with complex magnetic fields”, *Mon. Not. R. Astron. Soc.* **408** (2010) 2083–2091; doi:10.1111/j.1365-2966.2010.17284.x.
- [14] M. M. Mac Low and R. McCray, “Superbubbles in disk galaxies”, *Astrophys. J.* **324** (1988) 776–785; doi:10.1086/165936.
- [15] K. O. Mikaelian, “Rayleigh–Taylor and Richtmyer–Meshkov instabilities and mixing in stratified cylindrical shells”, *Phys. Fluids* **17** (2005) 094105; doi:10.1063/1.2046712.
- [16] M. Perucho and V. Bosch-Ramon, “On the interaction of microquasar jets with stellar winds”, *Astron. Astrophys.* **482** (2008) 917–927; doi:10.1051/0004-6361:20078929.
- [17] A. C. Raga, J. Cantó, A. Rodríguez-González and A. Esquivel, “Curved Herbig–Haro jets immersed in a stellar wind”, *Astron. Astrophys.* **493** (2009) 115–118; doi:10.1051/0004-6361:200810900.
- [18] S. W. Stahler and F. Palla, *The formation of stars* (Wiley, Berlin, 2004).